

# Final Report

To the

## Center for Highway Pavement Preservation (CHPP)



### Investigating Merits of Bio-Rejuvenation to Extend Pavement Service Life

for period

September 30, 2018

from

**Principal Investigator:** Ellie H. Fini, Ph.D., P.E.

E-mail: [elifini@gmail.com](mailto:elifini@gmail.com)

**Collaborator:**

Mehdi Zadshir

[m.zadshir@gmail.com](mailto:m.zadshir@gmail.com)

## **Executive Summary:**

The project studied merits of using various bio-rejuvenators as sprayed-on fog sealant to extend pavement service life by delaying pavement degradation, which is commonly occurred due to oxidation and UV aging. Accordingly, we evaluate how various bio-modifiers applied on the surface of pavement (bituminous materials) can delay aging specifically those caused by ultraviolet (UV) radiation during pavement service life. We further examined the differential effect of UV rays and oxidation on multiple bio-rejuvenators derived from wood pellet (WP), miscanthus (MS), corn stover (CS), and animal waste (BB). All samples were exposed to oxidative-aging and ultraviolet irradiation (UV-aging) individually. Oxidative aging was done in a rolling thin film oven followed by a pressurized aging vessel (PAV); UV-aging was performed under an ultraviolet irradiation machine that simulates the effect of sunlight. The chemical behavior of all specimens was evaluated using UV-vis absorption and Fourier Transform Infrared spectroscopy (FTIR). Thermal performance and rheological analysis were performed with differential scanning calorimetry (DSC) and dynamic shear rheometer (DSR), respectively. Thin Layer Chromatography with Flame Ionization detection (TLC-FID) was utilized for evaluating aging condition on the asphalt fractions. The average molecular weight was obtained by Gel Permeation Chromatography (GPC). Overall, the four types of bio-modified binders showed different sensitivity (e.g., aging indices) to the two aging conditions (i.e., UV-aging or oxidative-aging) while all performed better than scenarios without sprayed-on fog sealant. For UV-aging, MS showed least susceptibility to aging while in oxidative-aging, CS had the least aging susceptibility. FTIR results showed that carbonyl index increased after either oxidative-aging or UV-aging for all samples; however, the increase in carbonyl index was found to be more noticeable after UV-aging which was attributed to formation of free radicals accelerating oxygenation of carbon sites.

All four modifiers used as sprayed-on sealant found to be effective to protect underlying layers against oxidative-aging and UV-aging.

**Acknowledgement:** This research is sponsored by the University Transportation Center: Center for Highway Pavement Preservation and supervised and led by Dr. Fini (the PI). The research activities were performed by Mehdi Zadshir with assistance of several collaborators. The work would not be possible without the support from Columbia University, University of Illinois Urbana-Champaign and Illinois Sustainable Technology Center. The work led to two articles; one published at ASCE Journal of Materials and one was accepted by the Transportation Research Board Conference. The content of the report presented here is from aforementioned two papers.

Zadshir, M., Sh. Hosseinneshad, R. Ortega, F. Chen, D. Hochstein, J. Xie, H. Yin, M. M. Parast, and E. H. Fini, 2018, Application of a Bio-Modifier as Fog Sealant to Delay Ultraviolet (UV) Aging of Asphalt Binder and Crack Sealant, Journal of Materials in Civil Engineering, Volume 30 Issue 12 - December 2018.

Hosseinneshad, Sh., M. Zadshir, X. Yu, H. Yin, B.K., Sharma, and E. Fini, 2018, Differential Effect of UV-aging and Oxidative-aging on Bio-Modified Binders, Transportation Research Board (accepted)

## INTRODUCTION

Asphalt binder from petroleum resources has been widely used in pavement construction.

According to the National Asphalt Pavement Association (NAPA), of the 2.6 million miles of paved roads and highways in the US, over 94% are paved with petroleum-based asphalt (NAPA,2018). Asphalt binder in road construction serves as a waterproof and binding agent, and it is continuously exposed to oxidation and UV aging. Oxidation of asphalt components gradually alters asphalt thermo-mechanical properties. The degree of aging varies depending on service life, environmental conditions, and composition of the starting material (Petersen et al., 2009, Glover et al., 2009).

Different accelerated aging methods have been designed to simulate aging process that occurs in the field. The Rolling Thin Film Oven (RTFO) test is used to simulate the short-term oxidative aging that occurs during the mixing and compaction process, Pressure Aging Vessel (PAV) is used to simulate the long-term aging occurring during service life of the asphalt binder. However, in the field, the aging process of asphalt is not limited to the above processes and it involves a set of factors including solar radiation. Ultraviolet light which is part of solar radiation can be absorbed by asphalt surface to trigger chemical reactions resulting in acceleration of aging process. Some attempts have been done to evaluate UV-aging in laboratory (Durrieu et al., 2007). Wu et al compared the effects of laboratory simulated UV-aging with field aging, and their results showed UV-aging mainly happened in a thin top layer of binder, but its effect was more dominant than thermal aging (Wu et al., 2008). Although UV aging may not affect the entire bulk, excessive surface aging can promote raveling and crack initiation leading to top-down cracking (Fischer et al., 2015). Mechanism of aging and its effect on thermo-mechanical properties of asphalt binder is

very much impacted by its chemical composition; as such the aging process in asphalt binders made from petroleum resources may be different from those of bio-based binders.

In recent years, the use of bio-based binders in asphalt industry has been promoted. The current reduction of supply of quality asphalt combined with high demand for asphalt binder emphasize the need for alternative non-petroleum supply of asphalt binder to not only address the above concerns, but also improve pavement sustainability. On the other hand, the depletion of petroleum-based asphalt, price instability, and advancement in refineries motivated attempts to find alternative renewable asphalt resources from biomass (Podolsky et al., 2016). It should be noted that the main focus on the conversion of biomass has been to produce fuel; thermochemical processes such as hydrolysis, pyrolysis, gasification and liquefaction are used to convert biomass into biofuel (Pandey et al., 2015). Different feedstocks were used for biofuel production, and it was shown that biomass are promising sources for fuel production (Oasmaa et al., 2010).

However, more recently research on the use of biomass to produce bio-asphalt as replacement or partial replacement for asphalt binder has received more attention. Different studies examined merits of using non-petroleum resources such as woody biomass, waste cooking oil, algae oil, and animal waste to produce alternative bio-binder (Yang et al., 2013., You et al., 2011; Raouf et al., 2010; Chailleux et al., 2012; Fini et al., 2011). Raouf and Williams investigated the physical and chemical properties of bio-oils derived from oakwood, corn stover, and switch grass and reported that addition of their bio-oils to asphalt binder increased stiffness and high temperature properties of base asphalt (Raouf et al., 2010). Chailleux et al performed research on bio-oil derived from microalgae and showed their bio-oil has similar temperature dependency as asphalt binder; they concluded that their bio-oil from microalgae could be a promising candidate for use in asphalt

(Chailleux et al., 2012). Fini et al showed that bio-binder made from swine manure can enhance cracking resistance of asphalt binder (Fini et al., 2011). Even though the performance of bio-binder in terms of rheological and mechanical properties has been studied, there is no study on differential effects of various aging condition on bio-binders.

Accordingly, this paper studies effect of both oxidative-aging and UV-aging on the performance and durability of bio-modified asphalt by examining its physicochemical and rheological properties.

## **EXPERIMENT PLAN**

### **Materials**

The base binder used in this study was PG64–22, which is commonly used in the US. Bio-binder (BB) was made from swine manure using hydrothermal liquefaction in North Carolina A&T State University (Fini et al., 2011). Bio-oils including wood pellet (WP), Corn stover (CS), Miscanthus (MS) were produced from pyrolysis of biomass in Illinois Sustainable Technology Center at UIUC.

### **Bio-Modified Binders**

Bio-modified Binders were produced by blending each bio-oil with neat asphalt binder. BB, WP, CS, and MS, were blended at 10% by the weight of asphalt binder at 135°C for 30 minutes using a bench top shear mixer at the speed of 750 rpm.

### **Sample Preparation**

#### **UV-aging**

Sample for UV aging were prepared according to ASTM D1669, and conditioned using a QUV accelerated weathering machine following ASTM D4799. In this study, asphalt binder was placed at the bottom of the QUV machine under continuous UV exposure for 100 hours at a radiation intensity of  $0.89 \text{ W/m}^2 \cdot \text{nm}$  and a temperature of  $45^\circ\text{C}$ . Figure 1 shows the UV-aging machine loaded with bio-modified asphalt samples and the sample plate.

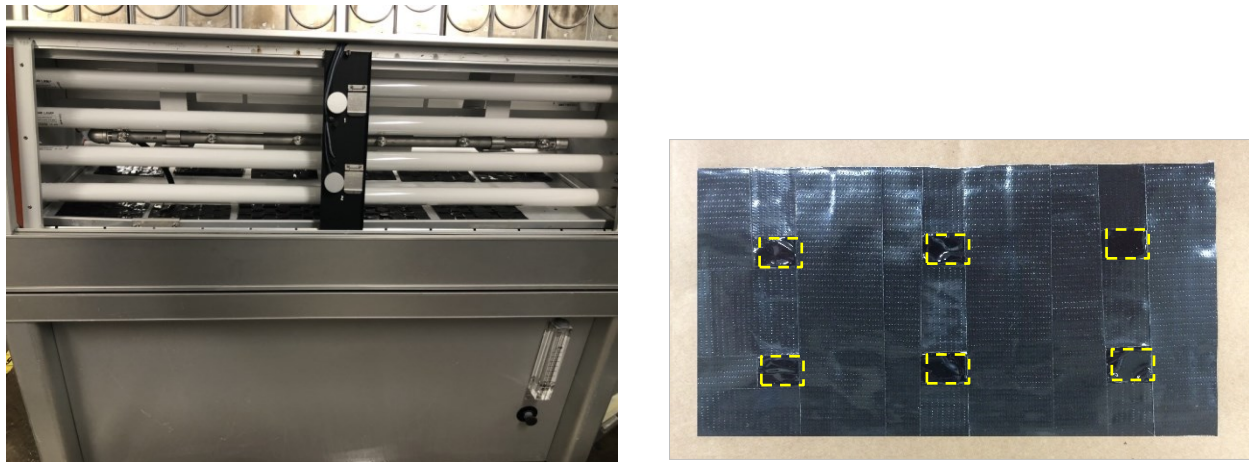


**FIGURE 1 QUV accelerated aging instrument (left), and prepared sample plate (right).**

### **Pressure Aging Vessel (PAV)**

Oxidative aging was performed following ASTM D2872, in which samples were subjected to the Rolling Thin Film Oven (RTFO) aging at  $163^\circ\text{C}$  and airflow of  $4 \text{ L/min}$  for 85 min. These RTFO samples were then exposed to PAV aging according to ASTM D6521. To do so, 50g of each RTFO-aged sample was subjected to a  $2.1 \text{ MPa}$  pressure at  $100^\circ\text{C}$  for 20 h.

### **Dynamic Shear Rheometer (DSR)**

To evaluate rheological properties of the bio-modified binders at medium to high temperatures, a Bohlin Gemini II dynamic shear rheometer (DSR) from Malvern Instruments was used with 25mm

parallel plates. This instrument can be operated within the range of room temperature to 300°C. In this study, frequency sweep test (0.1 to 100 rad/second) at 1% strain was performed at a temperature range of 34°C to 88°C with a 6°C interval. A residence time of 300 seconds was used before each test to ensure the sample has reached a steady temperature. The test results were used to calculate complex modulus, complex viscosity, and phase angle.

### **Attenuated Total Reflectance Fourier Transform Infrared Spectroscopy (ATR-FTIR)**

The Thermo Scientific Nicolet iS10 FT-IR Spectrometer was used in absorbance mode to acquire the spectra of each sample to analyze the effect of aging on chemical structure of bio-modified asphalt binders. Wavenumbers ranging from 4000 $\text{cm}^{-1}$  to 400 $\text{cm}^{-1}$  were covered. The background spectrum was taken after cleaning the diamond prism with methylene chloride for each sample. For quantitative analysis, structural indices are calculated according to Equations 1-4 (Yao et al., 2013).

$$I_{\text{C=O}} = \frac{\text{Area of carbonyl bond around } 1700 \text{ cm}^{-1}}{\text{Area of the spectral bonds between } 600 \text{ and } 2000 \text{ cm}^{-1}} \quad (1)$$

$$I_{\text{S=O}} = \frac{\text{Area of sulphoxide bond around } 1030 \text{ cm}^{-1}}{\text{Area of the spectral bonds between } 600 \text{ and } 2000 \text{ cm}^{-1}} \quad (2)$$

$$I_{\text{Ar}} = \frac{\text{Area of aromatic bond around } 1601 \text{ cm}^{-1}}{\text{Area of the spectral bonds between } 600 \text{ and } 2000 \text{ cm}^{-1}} \quad (3)$$

$$I_{\text{Al}} = \frac{\text{Area of aliphatic bond around } 1460 \text{ cm}^{-1}}{\text{Area of the spectral bonds between } 600 \text{ and } 2000 \text{ cm}^{-1}} \quad (4)$$

### **UV-Vis absorption spectroscopy**

Samples of asphalt binder were dissolved in chloroform. Absorption spectra were collected for these binder solutions using a quartz cuvette with 1 cm path length (28B-Q-10, Starna Cells) in the range of 300 – 800 nm on a Cary 6000i UV-Vis-NIR spectrophotometer (Varian). Based on



Equation 5, absorbance  $A$  at a specific wavelength  $\lambda$  is related to incident intensity  $I_o$ , transmitted intensity  $I$ , solution concentration  $c$ , pathlength  $l$ , and absorption coefficient  $\varepsilon$  according to the Beer-Lambert law for dilute solutions ( $A < 1$ ) (Lambert et al., 2011).

$$A_{\lambda} = \log \frac{I_o}{I} = \varepsilon_{\lambda} c l \quad (5)$$

The absorption spectrum around 800 nm which was close to zero was used as a reference to monitor and correct for excessive background noise for each sample. For qualitative analysis the absorbance of UV light at 300 – 400 nm and visible light at 400 – 700 nm were integrated from the UV-Vis spectra and visible/UV absorption ratio  $R_{vis/UV}$  was used to characterize the shape of the absorption curve (Equation 6). The selected measurement was found to be appropriate to distinguish between samples with different aging level. Aging index was calculated using Equation 7.

$$R_{vis/UV} = (\int_{400}^{700} Absorbance)_{vis}/300nm / (\int_{300}^{400} Absorbance)_{UV}/100nm \quad (6)$$

$$Aging\ Index = \left( \frac{Aged\ value - Unaged\ value}{Unaged\ value} \right) * 100 \quad (7)$$

### **Differential Scanning Calorimeter (DSC)**

TA Instruments Q250 Differential Scanning Calorimeter (DSC) was used to examine thermal properties of each specimen after exposure to oxidative-aging and UV aging. Specifically, Glass transition temperature,  $T_g$ , and specific heat capacity,  $C_p$  were calculated for each sample. For sample preparation, Tzero hermetic pans and hermetic lids were used to hold 10-20 mg of binder samples. No further drying process was applied to the binder samples before sealing the pan. The modulated DSC (MDSC) function was employed due to its higher sensitivity than regular DSC.

The method properly differentiates between reversing and non-reversing thermal behaviors in materials (Masson et al 2002). MDSC heating and cooling curves were obtained at different rates with a modulation period of 60s and an amplitude of  $\pm 0.47^{\circ}\text{C}$ . A nitrogen cooling system was used for cooling; nitrogen gas was purged at a rate of 50 ml/min. All samples were subjected to the following thermal cycles: (i) initial rapid cooling from  $120^{\circ}\text{C}$  to  $-80^{\circ}\text{C}$  at a ramp rate of  $10^{\circ}\text{C}/\text{min}$  followed by isothermal condition for 5 mins; (ii) first heating cycle from  $-80^{\circ}\text{C}$  to  $120^{\circ}\text{C}$  at  $4^{\circ}\text{C}/\text{min}$  followed by isothermal condition for 5 mins; (iii) cooling from  $120^{\circ}\text{C}$  to  $-80^{\circ}\text{C}$  at  $4^{\circ}\text{C}/\text{min}$  followed by isothermal condition for 5 mins; (iv) second heating cycle from  $-80^{\circ}\text{C}$  to  $120^{\circ}\text{C}$  at  $4^{\circ}\text{C}/\text{min}$  followed by isothermal condition for 5 mins.

#### **Thin-Layer Chromatography with Flame Ionization Detection (TLC-FID)**

To study the effect of the aging on the fractional composition of bio-modified binders, an Iatroscan MK-6s model TLC-FID analyzer was utilized. The hydrogen and air flow rate were set to 160 mL/min and 2 L/min, respectively. To separate asphaltene, 100 mL heptane per gram of asphalt was added into an Erlenmeyer flask with a stir bar. It was heated at a rolling boil with a condenser for 20 minutes followed by cooling for 1hr. Vacuum filtration was then performed for separating asphaltene followed by drying the precipitant for 15 minutes at  $110^{\circ}\text{C}$ . The precipitant was then weighed to obtain the percentage of asphaltene. After separation of asphaltene (n-heptane insoluble), 20  $\mu\text{g}$  of maltene (n-heptane soluble) was spotted on the chromrods. Dried chromrods were developed in a pentane tank for 35-40 minutes. After drying in air for 2-5 minutes, the chromrods were transferred into a second developing chamber filled with 9:1 toluene:chloroform solution for 9 minutes. After drying the rods in the oven at  $85^{\circ}\text{C}$ , the chromrods were scanned for 30s utilizing an Iatroscan with FID detector.

### Gel Permeation Chromatography (GPC)

Gel permeation chromatography was used to measure the average molecular weight. In GPC analysis, the separation of a macromolecules mixture takes place in the column; analytes are separated based on their sizes. As the solution goes through the column which is packed with fine, porous beads some particles enter into the pores. The smallest particles diffuse into all pores and have larger retention time, the medium particles access some pores, and the largest molecules are excluded from most pores eluting from the column faster than others.

GPC system consisted of a Waters 2695 separation module (equipped with system controller, multi-solvent delivery system, and autosampler) connected to two Styragel HR1 SEC columns (7.8mm × 300mm) in series followed by Waters 2414 RI detector and a computer with Empower Pro system control and data acquisition software. Samples of 3% w/w were prepared in tetrahydrofuran (THF) and were filtered using a 0.45 µm Millipore PTFE syringe filter to remove suspended particulates. THF was used as the carrier solvent with flow rate of 1.0 ml/min and injection volume of 20 µL. A constant flow of fresh eluent was supplied to the column via a pump to detect analytes.

The resulting chromatographic data was processed using Matlab through Equation 2 and 3. The weight-average molecular weight ( $M_w$ ) were calculated based on the component molecular weights ( $M_i$ ) determined from the retention time calibration curve and signal intensities ( $N_i$ ).

$$M_w = \frac{\sum M_i^2 N_i}{\sum M_i N_i} \quad (8)$$

## RESULTS AND DISCUSSION

### Chemical Analysis:

Effect of oxidative-aging and UV-aging on chemical functional groups of each specimen was tracked using an FTIR-ATR (Figure 2). It should be noted that understanding chemical functional groups of each bio-oil and the changes that occur in bio-modified binder after either of oxidative-aging or UV aging is essential for predicting their performance (Hosseinneshad et al., 2015).

As it can be seen in Figure 2a, FTIR spectra of three plant-based bio-oils have some similarities; one of the most noticeable functional groups observed for plant-based bio-oils in the area of 1100-1300  $\text{cm}^{-1}$  are related to aromatic and phenolic stretching; these groups showed a broad peak in all three plant-based bio-oils.

The two obvious peaks in plant-based bio-oils was around 1040-1200  $\text{cm}^{-1}$  which is related to C-O group of ether or alcohols, while for bio-binder from swine manure (BB) very low intensity peak was observed in that area. Also, the peak around 1514-1560  $\text{cm}^{-1}$  attributed to aromatic C=C ring stretching had lower intensity in the BB and higher intensity in the three plant-based bio-oils. Understanding chemical functional groups of bio-oils helps determine sensitivity of each bio-modified binder to a specific aging condition.

Carbonyl and sulfoxide indices have been used to track extent of aging in binder by many researchers (Dorrence et al., 1974); the change in carbonyl and sulfoxide content is an indicator of the change in physical properties of asphalt (Dorrence et al., 1974; Liu et al., 1996; Petersen et al., 2009). Figure 2b through 2d shows the spectra of all bio-modified binders before aging, after UV-aging, and after oxidative-aging, respectively. For unaged neat binder, carbonyl functional group C=O at 1700  $\text{cm}^{-1}$  was not detected while in binder containing plant-based bio-oil, this peak was noticeable mainly due to high oxygenated compounds in plant-based bio-oils (Yang et al., 2017).

This peak was not as strong for binder containing animal-based bio-oil compared to plant-based bio-oils, which indicates lower amount of carbonyl containing compounds in animal-based bio-oil than plant-based bio-oil.

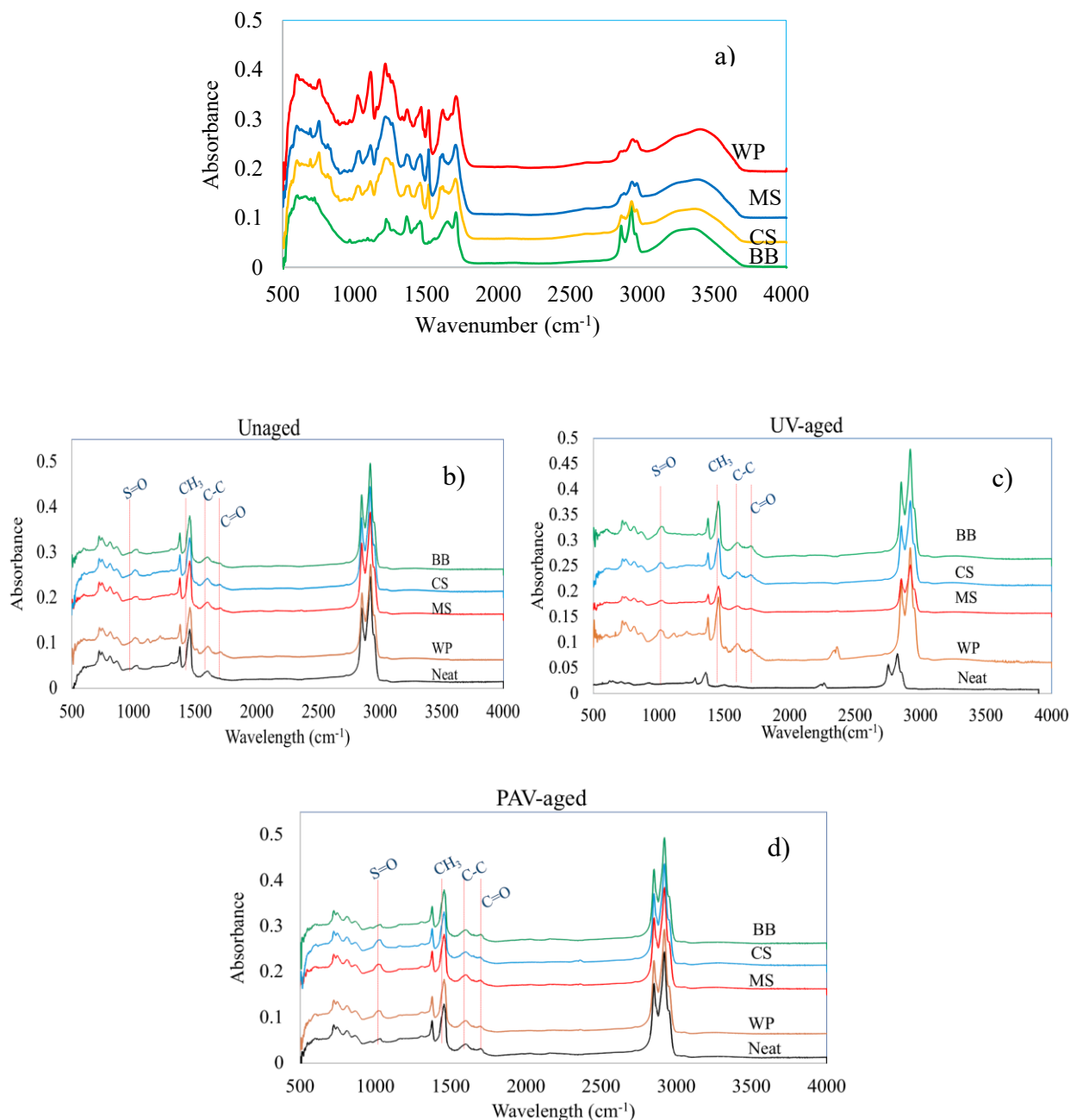


**FIGURE 2 a) FTIR spectrum of all pure bio-oils, b) spectra of bio-modified binders before aging c) after UV-aging and d) after oxidative-aging (PAV).**

To quantify changes in chemical functional groups due to oxidative aging and UV-aging, chemical structural indices (C=O, S=O, Aromatic, Aliphatic) were calculated using Equation 1 through 4 for each bio-modified binder. For unaged binder, carbonyl peak could not be detected.

The mechanism of UV-aging is based on photo-oxidation reaction; UV light catalyzes the reaction taking place within the top few micrometers of the exposed binder film (Zeng et al., 2018; Hu et al., 2018).

Higher carbonyl index for UV-aged bio-modified binders than asphalt binder suggests higher reactivity of free radicals toward oxygenation and formation of C=O groups. These free radicals may involve other reactions resulting in breakage of hydrocarbon side chains, and consequently reducing aliphatic content.

Bio-modified binders exposed to oxidative aging (PAV) show significantly lower carbonyl index than those exposed to UV-aging.

Sulfoxide index showed higher value for samples exposed to oxidative-aging than those exposed to UV-aging. Previous study by Peterson et al showed that sulfoxides and carbonyl are formed at different rates and the ratio of carbonyl to sulfoxide is related to the source of the asphalt binder (Petersen et al., 2011). With the same token, bio-modified binders due to different source of bio-oils showed variation in carbonyl and sulfoxide indices. It appears that during the UV-aging photo-generated free radicals attack carbon atoms to prompt carbonyl group formation, while oxidative aging was more effective in oxidizing the sulfur content.

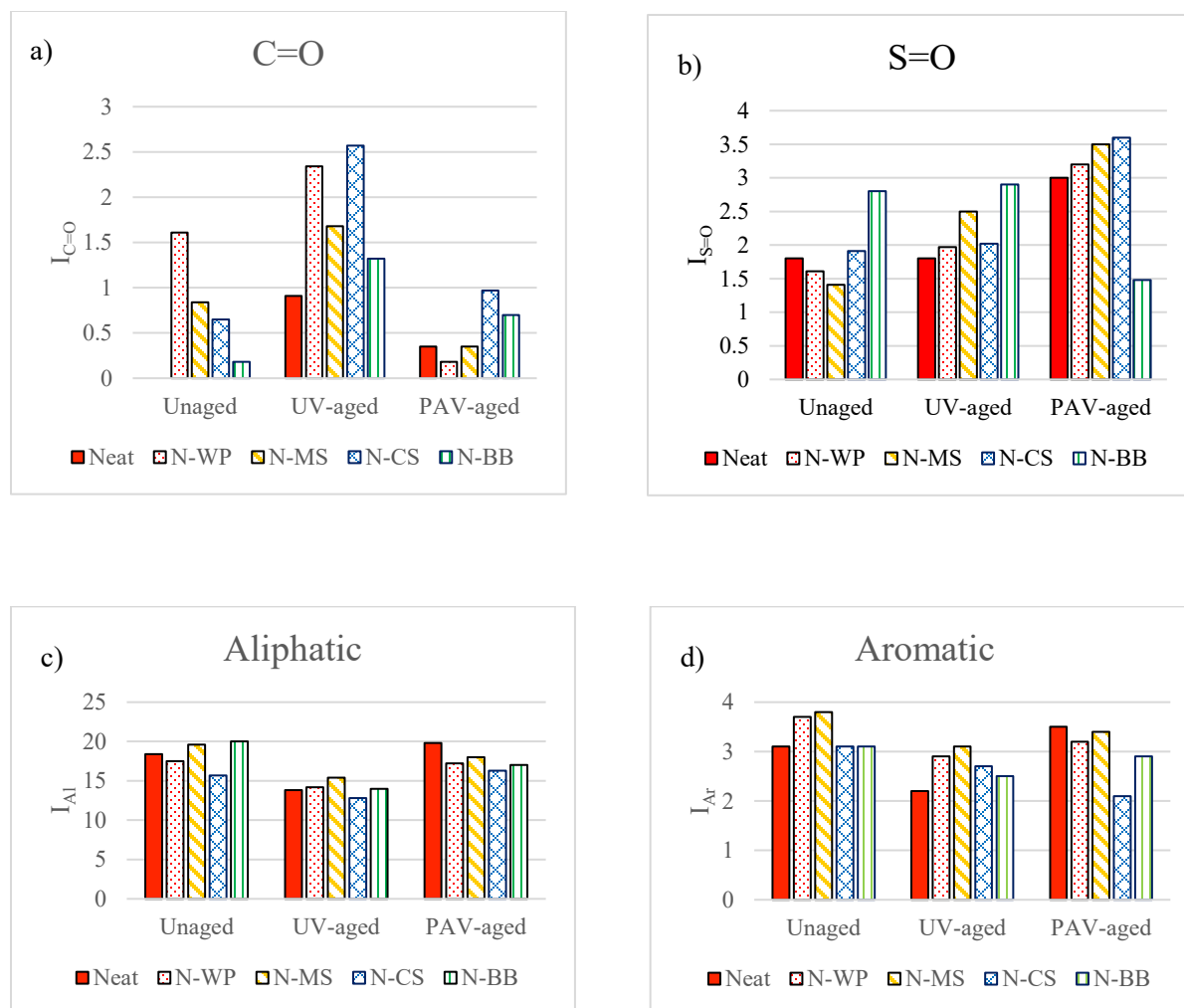


**FIGURE 3 a) Carbonyl index, b) sulfoxide c) Aliphatic, and d) aromatic index for neat and bio-modified binders before aging, after UV-aging, and oxidative aging (PAV).**

Effect of aging on the structural changes of bio-modified binders were investigated from absorbance of binders through UV-Vis spectra. Figure 4 shows spectra of unaged, UV-aged, and oxidative-aged specimens. Table 1 shows the structural index based on the summary of absorbance in visible area divided by the absorbance in UV area.

The UV spectrum can show the presence of specific bonding arrangements in the molecules; it has an advantage of the structural selectivity based on characteristic features or bonding arrangements. Any change in the structure of binder can shift the absorbance wavelength. Overall, increasing conjugation results in the shift of the UV-vis absorbance towards longer wavelength and consequently an increase in  $R_{vis/UV}$  ratio (Friedel et al., 1951; Weishaar et al., 2003). Since saturates cannot be detected using the absorbance method, their loss during the aging cannot be accounted for in the R ratio; but the loss of some volatiles like small aromatics and plausible agglomeration can be reflected in an increase of the R ratio. As it can be seen from the results both oxidative-aging and UV-aging led to increase of the  $R_{vis/UV}$  ratio. However, the increase was more noticeable for oxidative-aging.

Higher R ratio for oxidative-aging can be attributed to increased agglomeration after oxidation due to an increase in polarity and electrostatic interaction between agglomerated chromophores, which shifts the absorbance to longer wavelength. Tracking the change in R ratio can help predict the microstructural behavior of asphalt binders. Previous studies showed that polar component can form agglomeration leading to change of microstructural behavior of asphalt binder (Petersen et al., 2009).

Based on R ratio, the aging index was obtained according to Equation 7. All bio-modified binders showed lower aging indices than the neat binder. These indices found to be different for UV-aging and oxidative-aging, indicating that bio-modified binders have different sensitivity to the type of aging. For UV-aging, MS was least susceptible to aging while in oxidative-aging, CS had the least aging susceptibility. These results are valuable in choosing the bio-modified binder based on the source of biomass and its application in asphalt. For instance, the least susceptible binders to UV-



aging are better candidate for the surface fog sealant, which is exposed more to the sun light during the pavement service life (Zadshir et al., 2018).

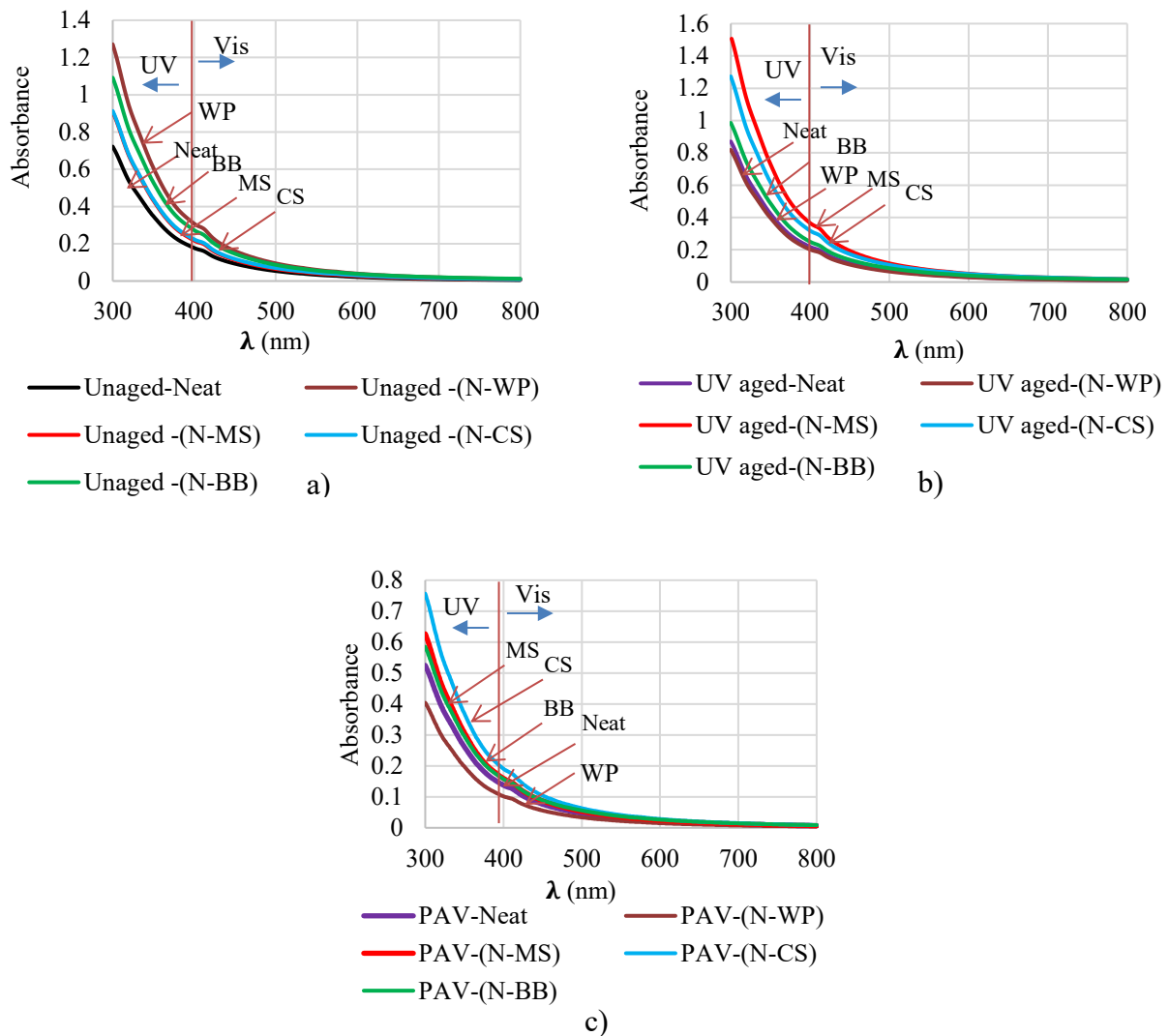


**FIGURE 4 Spectra of unaged, UV-aged, and oxidative-aged (PAV) of neat binder and bio-modified binders.**

**TABLE 1 Structural Index ( $R_{vis/UV}$ ) of Unaged, UV-aged, Oxidative-aged (PAV) for Neat binder, Bio-modified binders and Structural Aging Index**

Name of sample	Structural Index ( $R_{vis/UV}$ )			Structural Aging Index( $UV-Vis$ )	
	Unaged	UV-aged	PAV-aged	UV-aged	PAV-aged
Neat Binder	0.133	0.143	0.152	7.51	14.28
N-WP	0.134	0.141	0.146	5.22	8.95
N-MS	0.131	0.136	0.147	3.81	12.21
N-CS	0.138	0.146	0.146	5.79	5.79
N-BB	0.141	0.150	0.160	6.38	13.47

### DSC Analysis

The glass transition temperature ( $T_g$ ) of a material is related to its chemical compositional and structural changes (Masson et al., 2001; Masson et al., 2002); To study how different bio-oils and aging conditions affect the thermal properties of base binder,  $C_p$  at 30°C and  $T_g$  for all samples were determined from their corresponding second heating curves.

Figure 5 shows the  $C_p$  (at 30°C) and  $T_g$  values of the unaged, UV-aged, and oxidative-aged specimens. For unaged samples, the bio-modified binders had very similar specific heat capacity to that of the neat binder (within  $\pm 2\%$  of variation). Similar trend is seen in UV-aged samples – all five samples had comparable  $C_p$  values (within  $\pm 4\%$  of variation), which are also within  $\pm 3\%$  different from the specific heat of the unaged binders, indicating that 100-hour UV-aging did not change the specific heat capacity of the top layer of UV-aged samples. Oxidative aging reduced

the specific heat of the neat binder by 46%; however, it did not cause any significant changes in specific heat capacity of the bio-modified binders.

Since  $T_g$  is defined as the middle point of a temperature range where glass transition occurs, it is more appropriate to make qualitative (rather than quantitative) comparison among different samples. All bio-modified binders had lower  $T_g$  values than the neat binder, and this is independent of the aging process. The shift of  $T_g$  to lower temperature in bio-modified binders as compared to the neat binder may indicate that the bio-modified binders have enhanced cracking resistance at lower temperature compared to neat binder.

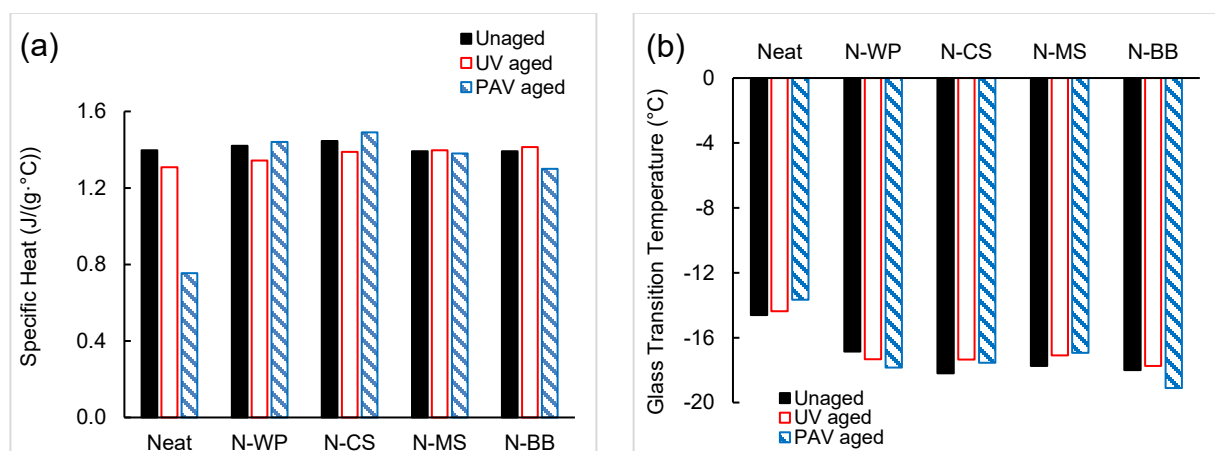


**FIGURE 5 Specific heat capacity at 30°C and glass transition temperature of all samples.**

For oxidative aged binders, all modified binders had  $C_p$  values 72% - 98% lower than the neat binder, indicating that all bio-modified binders effectively enhanced the oxidative aging resistance.

## TLC-FID Results

Result of SARA fractions are shown in table 2. Asphalt binder as a complex system is divided into four fractions of saturates, aromatics, resins, and asphaltenes. This fractionation is based on the solubility of each fraction in polar and non-polar solvents. Asphaltene fraction is insoluble in n-heptane and the soluble part is referred to as maltene including saturates, aromatics, and resins. In this system, the resins are peptizing the asphaltenes as absorbed on the outer layer of asphaltene micelles; while aromatics and saturates are inter-micellar continuous phase (Lesueur, et al, 2009). During the aging process, aromatics and resins are oxidized and behave more like asphaltene giving rise to asphaltene/resin ratio. This in turn disturbs stability of colloidal structure.

The colloidal stability index is defined by (Loeber et al, 1998) as:

$$CI = \frac{\text{resins} + \text{aromatics}}{\text{asphaltenes} + \text{saturates}} \quad (8)$$

Results of SARA fractions showed that all the unaged bio-modified binders had higher saturates, aromatics, and asphaltene content than the neat binder while they showed lower resin content than the neat binder. The percentage of asphaltene increased from 15.54% before aging to 28.23%, and 23.26% after UV-aging and oxidative aging, respectively. There was not significant increase in asphaltene fraction for all the bio-modified binders. The change in resin on the other hand was noticeable for all bio-modified binders, with significant amount of aromatics converting to resin due to aging. Increase in the resin fraction after UV-aging resulted in increase of the colloidal stability index. While colloidal stability for neat binder decreased 60% after UV-aging, colloidal stability of most bio-modified binder increased.

After oxidation aging, colloidal stability of neat binder reduced by 34%. The reduction was much lower for bio-modified binders indicating lower aging susceptibility. The reduction was lowest

for WP (3.3%) followed by BB (6.8%), MS (14%) and CS (18.6%). Overall, bio-modified binders found to be less susceptible to aging; In case, of UV-aging increase of resin content in bio-modified binder may further improve stabilization of the asphaltene molecules.

**TABLE 2 SARA Fractions of Unaged, UV-aged, Oxidative-aged (PAV) for Neat binder, Bio-modified binders**

	Name of Sample	Saturates	Aromatics	Resins	Asphaltene	CI
<b>Unaged</b>	Neat	9.22	29.54	45.69	15.54	3.03
	WP	14.92	31.75	32.45	20.87	1.79
	MS	11.64	31.45	38.63	18.26	2.34
	CS	10.87	32.55	36.76	19.81	2.25
	BB	11.84	32.67	34.49	20.98	2.04
<b>UV-aged</b>	Neat	16.94	26.31	28.49	28.23	1.21
	WP	10.3	22.63	46.06	21	2.19
	MS	8.81	25.86	46.06	18.52	2.63
	CS	10.27	22.21	46.08	21.42	2.15
	BB	8.23	23.6	47.25	20.9	2.43
<b>PAV-aged</b>	Neat	10.17	24.16	42.4	23.26	1.99
	WP	11.52	20.53	42.88	25.05	1.73
	MS	9.46	26.34	40.45	23.74	2.01
	CS	10.06	28.78	35.93	25.21	1.83
	BB	9.26	25.09	40.53	25.1	1.90

### **Average Molecular Weights**

The average molecular weight analysis shows a significant increase after aging with the effect of oxidative-aging being more significant than UV-aging. The observed significant increase in average molecular weight after oxidation aging is attributed to increased polarity giving rise to molecular association and agglomeration. The results are in accordance with the SARA fractions data showing a significant increase in asphaltene fraction after oxidative-ageing.

It should be noted that all bio-modified binders had higher molecular weight than neat binder before aging. It is in accordance with TLC-FID results, after modifying neat binder with bio-oils the asphaltene fraction increased in all bio-modified binders. Asphaltene are highly polar mixture of oxygen and/or nitrogen containing compounds with higher molecular weight. The association of small molecules with higher polarity results in higher molecular weight. Therefore, addition of bio-oil to neat binder increased the average molecular weight even before aging (Lu & Isacson, 2002).

After UV-aging, molecular weight of neat binder increased by 17.2% while the increase for WP, MS, CS, and BB was 2.3%, 2.9%, 6.5%, and 4.9%, respectively. After oxidative aging, molecular weight of neat binder was increased by 31%; while the increase for WP, MS, CS, and BB was 36.77%, 41%, 34.14%, and 34.83%, respectively.

**TABLE 3 Average Molecular Weight of Unaged, UV-aged, Oxidative-aged (PAV) for Neat and Bio-modified binders**

	Name of Sample	Average Molecular Weight (Da)	
Unaged	Neat	6234	Susceptibility to Aging (%)
	WP	7238	
	MS	6887	
	CS	7063	
	BB	6439	
UV-aged	Neat	7311	17.2
	WP	7405	2.3
	MS	7087	2.9
	CS	7524	6.5
	BB	6756	4.9
PAV-aged	Neat	8163	30.9
	WP	9900	36.7
	MS	9716	41
	CS	9475	34.1
	BB	8682	34.8

### DSR Analysis

Changes in the complex shear modulus ( $G^*$ ) as well as the phase angle of the neat and bio-modified binder before and after aging are shown in Figure 6. For all specimens, UV-aging has caused an increase in the modulus, resulting in stiffer samples. However, a much higher increase is observed in the  $G^*$  values of samples exposed to oxidative-aging than those exposed to UV-aging. The latter observation can be explained by aging mechanisms occur in each scenario. While UV rays mostly affect the surface of the samples and are less destructive to the bulk, constant diffusion of oxygen into the samples in a heated and pressurized vessel seems affects the entire bulk of the bio-modified binders, and consequently causing higher increase in bio-modified binders complex modulus values.

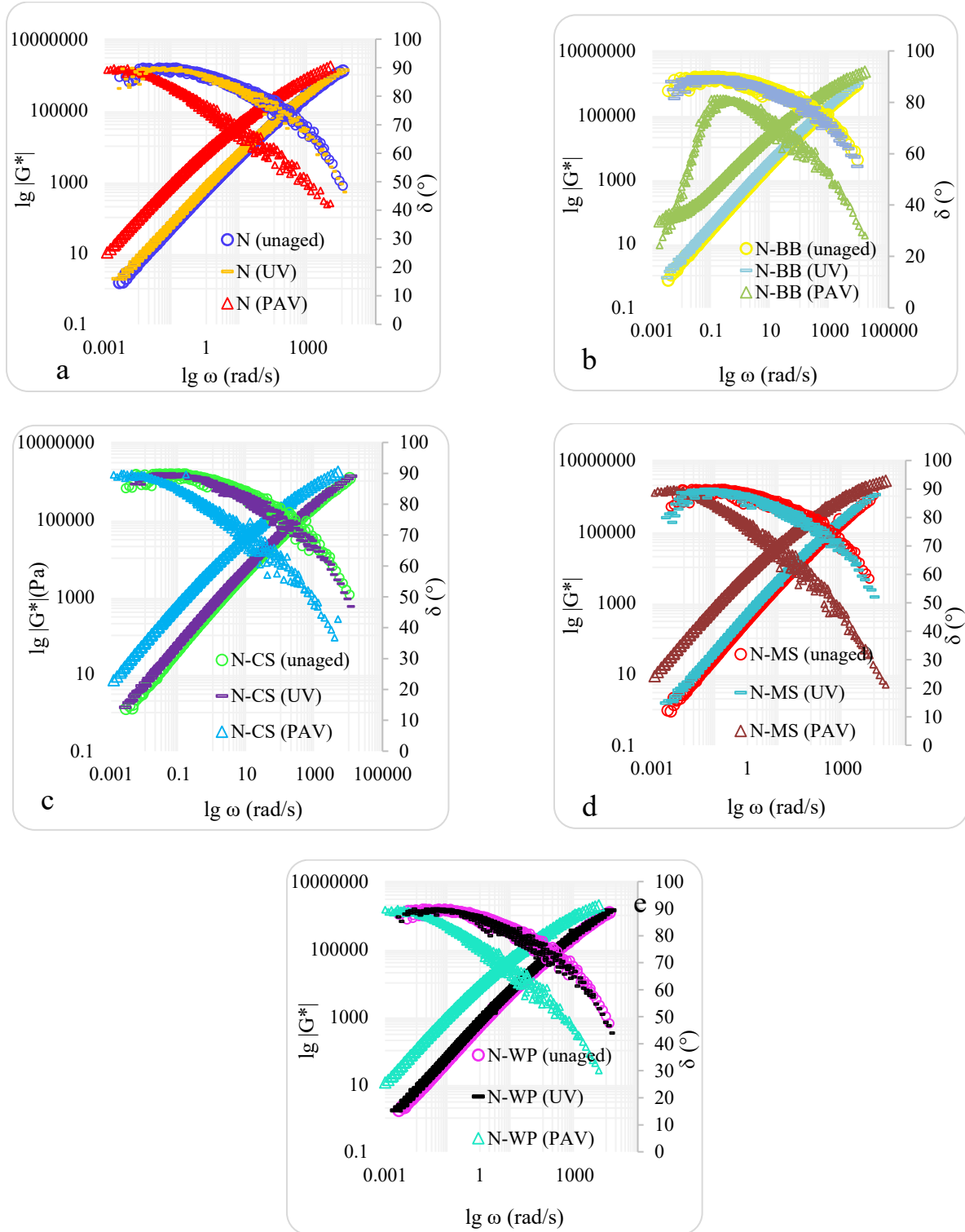


**FIGURE 6** Complex shear modulus and phase angle versus angular frequency of the samples.

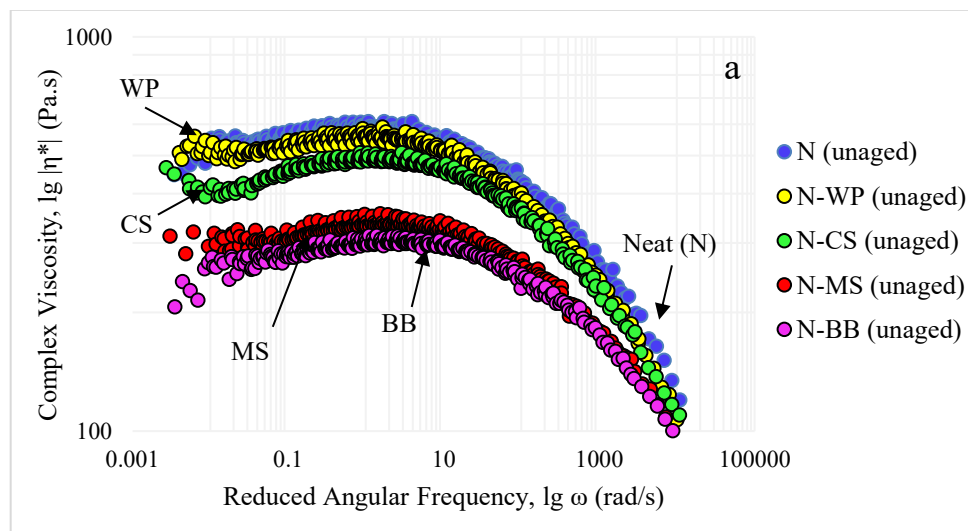


Figure 6 shows that complex shear and phase angle for the neat and modified binders

The average increase of complex modulus ( $G^*$ ) after UV-aging for WP, MS, CS, and BB were 20%, 34%, 28%, and 18.4% respectively. The increase in complex modulus after oxidative aging was significantly higher for all the modified binders which is related to higher effect of oxidative aging by constant diffusion of oxygen into the samples in a heated and pressurized vessel and consequently affecting the entire bulk. This increasing for complex modulus after oxidative aging was in average 153% for WP, 1221% for MS, 132% for CS, and 1009% for BB.

Figure 6 shows that for all the samples, at low frequencies (high temperatures), the oxidative- aged samples have a higher phase angle compared to UV aged samples.

It can be seen in Figure 7a that, the neat binder has the highest viscosity, and that adding the bio-oils reduces the viscosity of the binder, where BB shows the lowest viscosity among all. From Figure 7b, it can be concluded that exposure of the samples to the UV rays increases the viscosity of all samples. The highest increase is seen in the UV-aged MS samples with an average of 35.8% increase compared to the unaged one.



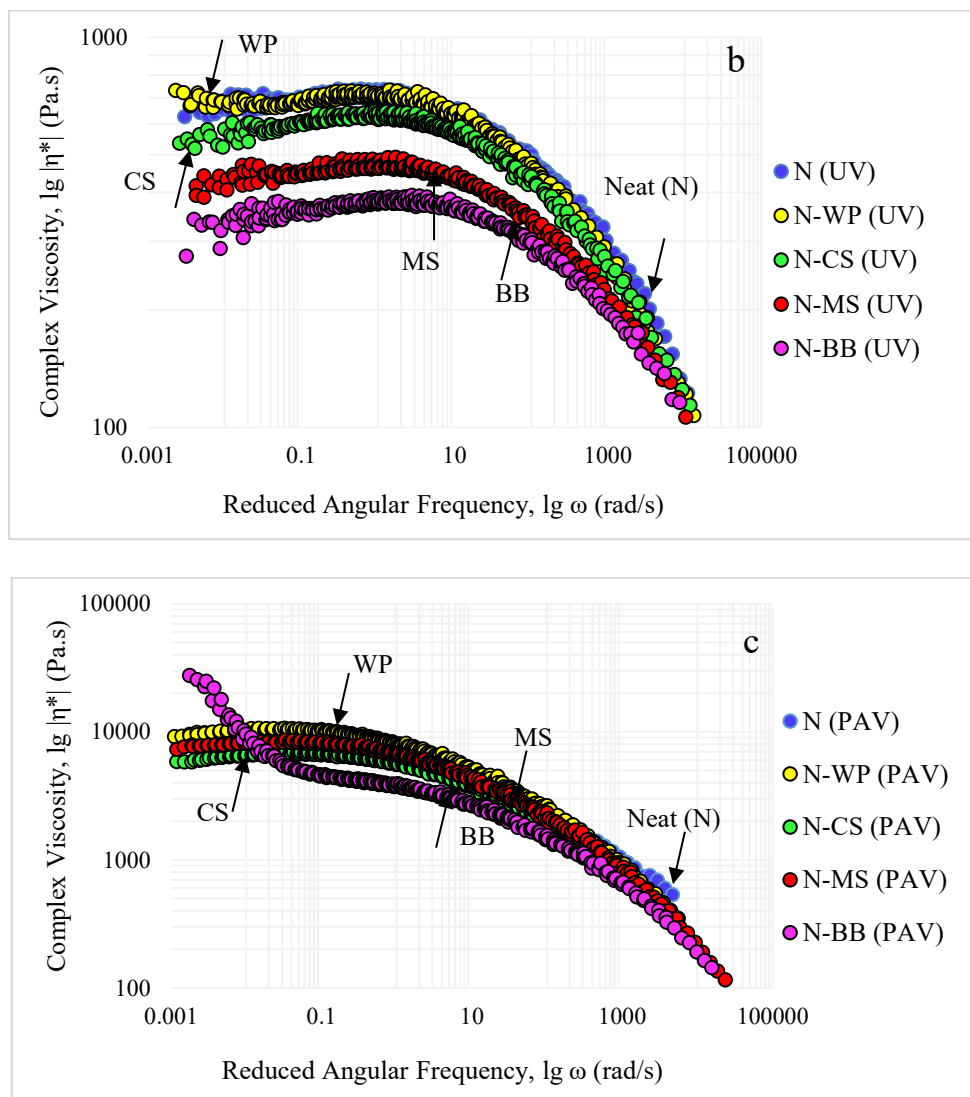


**FIGURE 7 Complex viscosity of a) unaged; b) UV aged, and c) oxidative aged (PAV) samples.**

## CONCLUSION

This study investigates differential effect of UV-aging and oxidative aging on the physicochemical and rheological properties of various bio-modified binders. The study results led to following conclusions:

- FTIR studies showed UV-aging has different aging mechanisms than oxidative aging; higher carbonyl index was observed in UV aged samples, while a higher sulfoxide aging index was observed in oxidative-aged samples. Reduction in aliphatic groups after UV-aging was more pronounced compared to oxidative aging.
- Carbonyl index and sulfoxide index for bio-modified binders was higher than neat binder even before aging, which can be related to presence of higher oxygenated compounds in bio-modified binder as evidenced by the FTIR spectra of bio-oils.
- Structural analysis using UV-Vis spectrometer and  $R_{vis/UV}$  ratio as a measure of aging showed all bio-modified binders were less susceptible to aging.  $R_{vis/UV}$  ratio of the same specimen found to be higher for oxidative-aging than for UV-aging. This in turn indicates that oxidative-aging can promote formation of conjugated structures and nano-aggregates, which consequently shifts the absorption to higher wavelength.
- Results of SARA fractions showed aging cause a significant increase in asphaltene fraction of neat binder while for bio-modified binder the main increase was observed in resin fraction. Accordingly, Colloidal stability index of neat binder showed 60% and 34 % reduction after UV-aging and oxidative aging, respectively. However, the reduction found to be much less for bio-modified binders with CS (18.6%) reflecting the highest among all bio-modified binders. In the case of UV-aging most bio-modified binders showed an increase in colloidal stability. This increase was the result of conversion of aromatics to resin giving rise to colloidal stability after UV-aging.
- GPC analysis showed both aging methods increased the average molecular weight. While bio-modified binders showed significantly lower susceptibility to UV-aging. Average molecular weight increased 17.27% for neat binder after UV-aging while it was 2.3%,

2.9%, 6.5%, and 4.9%. for WP, MS, CS, and BB respectively. The average molecular weight increased for all the specimens after oxidative aging, with BB and CS having less susceptibility to aging.

- Differential Scanning Calorimeter measurements showed that oxidative-aging reduced the specific heat capacity of the neat binder by 46%; while the change in the bio-modified binders was not significant. In addition, the glass transition temperature was reduced for all bio-modified binders independently of the aging type. This may indicate that all bio-modified binders could have better thermal cracking resistance than the neat binder.
- Complex modulus value showed higher increase after oxidative aging than UV-aging in all specimens. While UV aging mostly affects the surface of the samples and are less destructive to the bulk, oxidative aging affects the entire bulk by gradual diffusion of oxygen and progressive oxidation in bio-modified binders.

The outcome of this study shows differential effect of UV-aging and oxidative-aging on several bio-modified asphalt binders. Such differential effect is substantial when selecting bio-modified binders for special applications such as surface sealant or fog sealant in asphalt. Accordingly, bio-modified binders which are less susceptible to UV-aging are better candidates for pavement surface applications with significant exposure to sunlight during the pavement service life.

## REFERENCES

- Chailleux, E., Audou, M., Bujoli, B., Queffelec, C., Legrand, J., Lepine, O., (2012), Alternative Binder from Microalgae: Algoroute Project. Transportation Research E-circular, 7-14.
- Dorrence, S. M., Bartour, F. A., & Petersen, J. C. (1974), Direct evidence of ketones in oxidized asphalt, *Analytical Chemistry*, 46(14), 2242-2244.
- Durrieu F., Farcas F., Mouillet V. (2007), The influence of UV aging of a SBS modified bitumen: Comparison between laboratory and on site aging, *Fuel*, 86, 1446-1451.
- Fini, E., Kalberer, E., Shahbazi, A., Basti, M., You, Z., Ozer, H., Aurangzeb, Q., (2011), Chemical characterization of bio-binder from swine manure: sustainable modifier for asphalt binder. *J. Mater. Civ. Eng.* 23, 1506-1513.
- Fini, E. H., Al-Qadi, I. L., You, Z., Zada, B., & Mills-Beale, J. (2012), Partial replacement of asphalt binder with bio-binder: characterisation and modification. *International Journal of Pavement Engineering*, 13(6), 515-522.
- Friedel, R. A.; Orchin, M. (1954), *Ultraviolet spectra of aromatic compounds*. Wiley New York, 40.

Fischer, H. R., & Dillingh, B. (2015). Response of the microstructure of bitumen upon stress-damage initiation and recovery. *Road Materials and Pavement Design*, 16(1), 31-45.

Glover, C. J.; Martin, A. E.; Chowdhury, A.; Han, R.; Prapaitrakul, N.; Jin, X.; Lawrence, J. (2009), Evaluation of binder aging and its influence in aging of hot mix asphalt concrete: literature review and experimental design. (No. FHWA/TX-08/0-6009-1).

Hosseinnezhad, S., Fini, E. H., Sharma, B. K., Basti, M., & Kunwar, B. (2015), Characterization of Synthetic bio-oils produced from biomass: A sustainable source for construction bio-adhesive, *RSC Advances*, 5(92), 75519-75527.

Hu, J., Wu, S., Liu, Q., Hernandez, M. I. G., Wang, Z., Nie, S., & Zhang, G. (2018), Effect of ultraviolet radiation in different wavebands on bitumen. *Construction and Building Materials*, 159, 479-485.

Lambert, J. B.; Gronert, S.; Shurvell, H. F.; Lightner, D. A. (2011), *Organic Structural Spectroscopy*; 2nd ed.; Prentice Hall: New York.

Liu, M., Lunsford, K. M., Davinson, R. R., Glover, C. J., & Bullin, J. A. (1996), The kinetics of carbonyl formation in asphalt. *Alche Journal*, 42(4), 1069-1076.

Lesueur, D. (2009). The colloidal structure of bitumen: Consequence on the rheology and on the mechanism of bitumen modification, *Advances in colloid and interface science*, 145(1), 42-82.

Loeber., Muller, G., Morel, J., & Sutton, O. (1988). Bitumen in colloid science: a chemical structure and rheological approach, *Fuel*, 77(13), 1443-1450.

Lu, X., & Isacson, U. (2002). Effect of ageing on bitumen chemistry and rheology. *Construction and Building Materials*, 16(1). 15-22.

Masson, J. and G. Polomark, (2001). Bitumen microstructure by modulated differential scanning calorimetry. *Thermochimica acta*, 374(2), 105-114.

Masson, J., G. Polomark, and P. Collins, (2002). Time-dependent microstructure of bitumen and its fractions by modulated differential scanning calorimetry. *Energy & Fuels*, 16(2), 470-476.

National Asphalt Pavement Association, “Sustainable Asphalt, Now and Tomorrow” (visited July 25, 2018). <http://www.asphaltpavement.org>.

Oasmaa, A. Solantausta, Y. Arpiainen, V. Kuoppala, E. Sipila, K. (2010). Fast Pyrolysis Bio-Oils from Wood and Agricultural Residues. *Journal of Energy and Fuels*, 24, 1380-1388.

Oldham, D. J., E. H. Fini, and E. Chailleux. (2015). Application of a Bio-binder as a Rejuvenator for Wet Processed Asphalt Shingles in Pavement Construction, *Construction and Building Materials*, 86 (1), 75–84.

Pandey, A., Bhaskar, T., Stocker, M., Sukumaran, R., (2015). Advances in Thermo-chemical Conversion of Biomass Introduction, Recent Advances in Thermo- chemical Conversion of Biomass. Elsevier, Amsterdam, Netherlands, 3-30.

Petersen, J. C., (2009). A review of the fundamentals of asphalt oxidation: chemical, physicochemical, physical property, and durability relationships. In *Transportation Research E-Circular*, (E-C140).

Petersen, J. C., & Glaser, R. (2011). Asphalt oxidation mechanism and the role of oxidation products on age hardening revisited, *Road Materials and Pavement Design*, 12(4), 795-819.

Podolsky, J.H., Buss, A., Williams, R.C., Cochran, E., (2016). Comparative performance of bio-derived/chemical additives in warm mix asphalt at low temperature. *Mater Struct.* 49, 563-575.



Raouf, M.A., Williams, R.C., (2010). Rheology of fractionated corn stover bio-oil as a pavement material. *Int. J. Pavements*, 9, 58-69.

Weishaar, J. L., Aiken, G. R., Bergamaschi, B. A., Fram, M.S., Fujji, R., & Mopper, K. (2003). Evaluation of specific ultraviolet absorbance as an indicator of chemical composition and reactivity of dissolved organic carbon. *Environmental science & technology*, 37(20), 4702-4708.

Wu, S., Pang, Mo, L., Qiu, J., Zhu, G., & Xiao, Y. (2008). UV and thermal aging of pure bitumen-comparison between laboratory simulation and natural expose aging. *Road Materials and Pavement Design*, 2008. 9(sup1), 103-113.

Yang, X., You, Z., Dai, Q., (2013). Performance evaluation of asphalt binder modified by bio-oil generated from waste wood resources. *Int. J. Pavement Res. Technol.* 6, 431-439.

Yao, H., Z. You, L. Li, C. H. Lee, D. Wingard, Y. K. Yap, X. Shi and S. W. Goh (2013). Rheological properties and chemical bonding of asphalt modified with nanosilica. *Journal of Materials in Civil Eng.* 25(11), 1619-1630.

Yang, X., Mill-Beale, J., & You, Z. (2017). Chemical characterization and oxidative aging of bio-asphalt and its compatibility with petroleum asphalt. *Journal of cleaner production*, 142, 1837-1847.

You, Z., Mills-Beale, J., Fini, E., Goh, S., Colbert, B., (2011). Evaluation of low-temperature binder properties of warm-mix asphalt, extracted and recovered RAP and RAS, and bioasphalt. *J. Mater. Civ. Eng.* 23, 1569-1574.

Zadshir, M., Hosseinneshad, S., Ortega, R., Chen, F., Hochstein, D., Xie, J., Yin, H., Parast, M., Fini, E. H., (2018). Application of a Biomodifier as Fog Sealant to Delay Ultraviolet Aging of Bituminous Materials. *Journal of Materials in Civil Engineering*, 30(12), 04018310-1-12.

Zeng, W., Wu, S., Pang, L., Chen, H., Hu, J., Sun, Y., & Chen, Z. (2018). Research on Ultra Violet (UV) aging depth of asphalt. *Construction and Building Materials*, 160, 620-627.